could range from 10 to 100 MA.

Farther out one encounters minor swept-back and swept-forward signatures; however, beyond a radial distance of 38 R_J, the field lines adopt a systematic configuration, indicating that the magnetic field is swept toward the magnetotail. We suggest that this field configuration is due to an outflow resulting from equatorially confined material expanding into the magnetotail as it rotates from the dayside.

The Jovian magnetosphere and its neighboring regions are rich in low-frequency wave phenomena. Fluctuations in the interior of the magnetosphere extend to the time resolution of the instrument. Both transverse (Alfvén) and compressional magnetohydrodynamic waves have been detected. Waves were first detected upstream of the bow shock (foreshock) and then in the magnetosheath and the magnetosphere. Here we present only one set of observations from the outbound pass. In Fig. 4 we show the overview of the field magnitude for an entire day (12 February, 12:00 UT to 13 February, 12:00 UT), together with 1-s high-resolution data for a swathe of 1 hour. The structures are characterized by large variations in the ambient magnetic field magnitude (a factor of ~ 3 in this example), with little or no change in field direction. The structures are neither sinusoidal nor periodic; the time scale of fluctuation is about 1 to 2 min. These structures are believed to be nonoscillatory mirror-mode waves (*15*) and have previously been detected in Earth's and in Saturn's magnetosheath (*16*), as well as in interplanetary space (*17*). These are the longest lasting such wave trains observed in space.

REFERENCES AND NOTES

1. E. J. Smith, K.-P. Wenzel, D. E. Page, *Science* **257**, 1503 (1992).
2. A. Balogh *et al.*, *Astron. Astophys. Suppl. Ser.* **92**, 221 (1992). Information relevant to the encounter period is as follows: there are two triaxial magnetometer sensors on Ulysses; the background field at the location of the sensors is no more than 0.05 nT; the offsets of the two magnetometers are cross-calibrated to about 0.05 nT or better; vector measurements are made by the two magnetometers at the rate of one per second each; the measurements outside about 20 R_J were made by both magnetometers; the maximum field measured at closest approach was 2372 nT.
3. E. J. Smith, L. Davis, Jr., D. E. Jones, in *Jupiter*, T. Gehrels, Ed. (Univ. of Arizona Press, Tucson, 1976), p. 788.
4. M. H. Acuña, K.W. Behannon, J. E. P. Connerney, in *Physics of the Jovian Magnetosphere*, A. J. Dessler, Ed. (Cambridge Univ. Press, London, 1983), p. 1.
5. E. J. Smith *et al.*, *J. Geophys. Res.* **79**, 3501 (1974).
6. R. P. Lepping, L. F. Burlaga, L. W. Klein, *Geophys. Res. Lett.* **8**, 99 (1981).
7. E. J. Smith *et al.*, *Science* **188**, 451 (1975).
8. H. S. Bridge *et al.*, *ibid.* **204**, 987 (1979).
9. J. E. P. Connerney, *Planetary Radio Emissions Workshop* (Graz, Austria, in press).
10. V. M. Vasyliunas, in *Physics of the Jovian Magnetosphere*, A. J. Dessler, Ed. (Cambridge Univ. Press, London, 1983), p. 395.
11. J. E. P. Connerney, M. H. Acuña, N. F. Ness, *J. Geophys. Res.* **86**, 8370 (1981).
12. Current sheet models have been proposed by the following: C. K. Goertz, *ibid.* **81**, 3368 (1976); M. G. Kivelson, P. J. Coleman, Jr., L. Froidevaux, R. L. Rosenberg, *ibid.* **83**, 4823 (1978); V. M. Vasyliunas and A. J. Dessler, *ibid.* **86**, 8435 (1981); K. K. Khurana and M. G. Kivelson, *ibid.* **94**, 11791 (1989).
13. S.-Y. Su and B. U. O. Sonnerup, *Phys. Fluids* **11**, 851 (1968).
14. T. W. Hill, A. J. Dessler, C. K. Goertz, in *Physics of the Jovian Magnetosphere*, A. J. Dessler, Ed. (Cambridge Univ. Press, London, 1983), p. 353.
15. A. Hasagawa, *Physics and Chemistry in Space* (Springer Verlag, New York, 1975), vol. 8, p. 94.
16. B. T. Tsurutani *et al.*, *J. Geophys. Res.* **87**, 6060 (1982).
17. B. T. Tsurutani, D. J. Southwood, E. J. Smith, A. Balogh, *Geophys. Res. Lett.* **19**, 1267 (1992).

18. We thank the project, operations, and data system teams from the Jet Propulsion Laboratory (JPL) and the European Space Association for their roles in the successful flyby of Jupiter by Ulysses and the recovery of high-quality data; Project scientists K.-P. Wenzel, E. J. Smith, and R. G. Marsden for coordinating the science operations; and our colleagues in the other Ulysses instrument teams for enlightening discussions. Most of the early Ulysses magnetometer development program was carried out under the leadership of P. C. Hedgecock. We acknowledge the helpful contribution of J. E. P. Connerney to our implementation of his Jovian magnetic field model. The Imperial College contribution to Ulysses is supported by the U.K. Science and Engineering Research Council; some of the research reported here was carried out by the JPL, California Institute of Technology, under contract with the National Aeronautics and Space Administration.

1 June 1992; accepted 30 July 1992

The Hot Plasma Environment at Jupiter: Ulysses Results

L. J. Lanzerotti,* T. P. Armstrong, R. E. Gold, K. A. Anderson, S. M. Krimigis, R. P. Lin, M. Pick, E. C. Roelof, E. T. Sarris, G. M. Simnett, C. G. Maclennan, H. T. Choo, S. J. Tappin

Measurements of the hot plasma environment during the Ulysses flyby of Jupiter have revealed several new discoveries related to this large rotating astrophysical system. The Jovian magnetosphere was found by Ulysses to be very extended, with the day-side magnetopause located at $\sim$105 Jupiter radii. The heavy ion (sulfur, oxygen, and sodium) population in the day-side magnetosphere increased sharply at $\sim$86 Jupiter radii. This is somewhat more extended than the "inner" magnetosphere boundary region identified by the Voyager hot plasma measurements. In the day-side magnetosphere, the ion fluxes have the anisotropy direction expected for corotation with the planet, with the magnitude of the anisotropy increasing when the spacecraft becomes more immersed in the hot plasma sheet. The relative abundances of sulfur, oxygen, and sodium to helium decreased somewhat with decreasing radial distance from the planet on the day-side, which suggests that the abundances of the Jupiter-derived species are dependent on latitude. In the dusk-side, high-latitude region, intense fluxes of counter-streaming ions and electrons were discovered from the edge of the plasma sheet to the dusk-side magnetopause. These beams of electrons and ions were found to be very tightly aligned with the magnetic field and to be superimposed on a time- and space-variable isotropic hot plasma background. The currents carried by the measured hot plasma particles are typically $\sim 1.6 \times 10^{-4}$ microamperes per square meter or $\sim 8 \times 10^5$ amperes per squared Jupiter radius throughout the high-latitude magnetosphere volume. It is likely that the intense particle beams discovered at high Jovian latitudes produce auroras in the polar caps of the planet.

This report discusses the initial results obtained from measurements made by the HI-SCALE (heliosphere instrument for spectra, composition, and anisotropy at low energies) experiment as the Ulysses spacecraft traversed the Jovian magnetosphere. The primary objectives of the HI-SCALE investigation (*1*) at Jupiter are to make measurements of the hot plasma ($\gtrsim$40 keV and $\gtrsim$50 keV for electrons and ions, respectively) population, including spatial distributions and flows, and to characterize the composition of the hot plasma and energetic particle populations (*2*). Of particular interest are the plasma conditions and plasma physics of the high-latitude magnetosphere of this rapidly rotating astrophysical object that could be measured for the first time during the outbound Ulysses pass.

The HI-SCALE instrument (*3*) operated flawlessly throughout the encounter. During the one day around closest approach (day 39, 8 February 1992), the protective covers that are included on three of the particle telescopes were closed, and the entire instrument was turned off. The covers prevented the three non–foil-covered detectors from being implanted with the low-energy heavy ions in the magnetosphere, possibly producing damage or increased thresholds, or both.

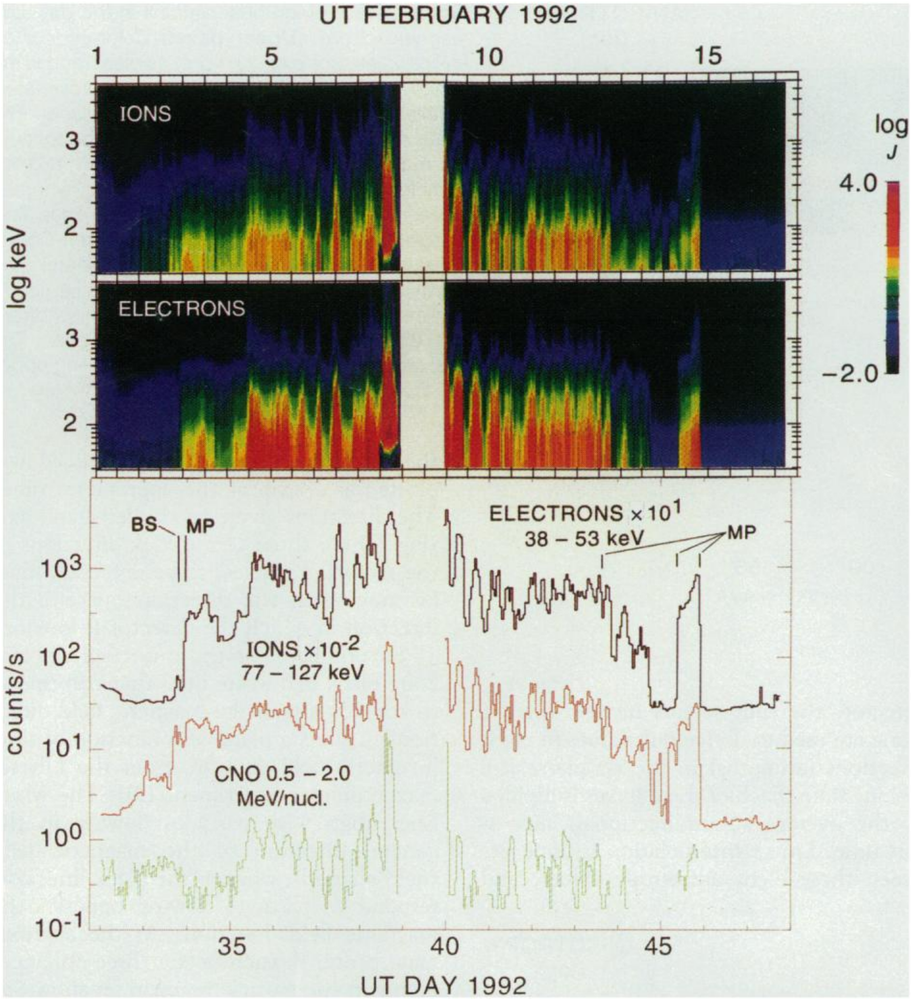

Fig. 1. Overview of HI-SCALE measurements of ions and electrons in Jupiter's magnetosphere. (**Upper panels**) Energy spectrograms of ions and electrons as a function of time during the encounter. The color-coded particle flux scale [particles/(cm^2 s sr keV)] is shown to the right of the panels. (**Lower panel**) Counting rates as a function of time during the encounter of two low-energy ion and electron channels and one broad energy channel of the sum of the CNO rates. The time of crossing of the day-side bow shock (BS) and magnetopause (MP) on day 33 inbound are noted, as are three of the magnetopause crossings on days 43 and 45 outbound. Nucl., nucleon.

As did the low-energy charged-particle (LECP) instrument on Voyager (*4*) (with particle energy ranges similar to those of HI-SCALE), our Ulysses instrument detected evidence of Jupiter's presence by means of sunward-flowing ions (*5*) substantially upstream of the planet (possibly as early as day 300 1991) (*6*). Such occurrences became more frequent as the spacecraft approached Jupiter. In energy spectrograms for the low-energy ions and electrons plotted as a function of time throughout the Jupiter encounter interval (Fig. 1), an approximate 10-hour periodicity is clearly evident in the enhancements of the fluxes, particularly in the 2 days before closest approach and in the day after closest approach. Plotted in the lower panel of Fig. 1 are hourly average counting rates of electron, ion, and CNO (carbon-nitrogen-oxygen) particles detected throughout the Jupiter encounter. After crossing the day-side magnetopause, the spacecraft did not exit it entirely again until some 10 days later (*7*).

The low-energy ion fluxes shown (Fig. 1) were enhanced around the time of the bow-shock crossing on day 33. The ion flux at this energy also increased by a factor of more than 50 several hours before the identified magnetopause crossing late on day 33. This crossing was sharply evident in the electron rates, which increased by a factor of nearly 100 at the time. The energetic CNO ions were also enhanced outside the magnetosphere on day 33. This enhancement was probably from a corotating interplanetary event, as Fe nuclei (*8*) were detected by the HI-SCALE instrument at this time. These heavy ion rates did not increase again substantially until about hour 8 on day 35 at ~86 Jupiter radii (R_J). After this time until the instrument was turned off, the CNO ion rates (principally oxygen inside the magnetosphere) clearly varied with an approximately 10-hour period. These enhancements in the fluxes of the heavier ions correspond to encounters of the spacecraft with the Jovian plasma sheet. Similar clear periodicities were not measured in the low-energy ion and electron channels until about the middle of day 36 at ~60 R_J.

After the spacecraft made its closest approach to the planet and the instrument was turned on on day 40, periodicities were again seen in the electron and ion rates for approximately 36 hours as Ulysses plunged through the dusk-side, high-latitude magnetosphere. CNO ions were rather sparse during much of the time immediately after the instrument was turned on. The electron and ion rates remained elevated and steady for nearly 2 days beginning during the later portion of day 41. The CNO ions were much more variable during this interval before the first outbound crossing of the magnetopause. The spacecraft solidly reentered the magnetosphere for about 12 hours on day 45 before leaving the magnetosphere for the last time.

As noted above, the HI-SCALE instrument measured features of the day-side plasma sheet during the inbound pass of Ulysses. Plotted in the lower panel of Fig. 2 are the count rates in two opposite angular sectors of one of the ion sensor heads that scans approximately in the equatorial plane of the planet (in the spacecraft x-z plane, where the $+z$ direction is pointed at the earth and the $+x$ axis is pointed approximately into the planet's local morning direction). The rates are larger for the ion fluxes incident into the sector looking into the $+x$ direction than for the sector looking into the $-x$ direction. That is, the higher fluxes of particles are moving toward $-x$, the direction expected of particles moving in the corotation direction of the planet (*4*). Furthermore, the anisotropies tend to be larger during the times of the flux enhancements, which correspond approximately to encounters with the day-side plasma sheet.

L. J. Lanzerotti and C. G. Maclennan, AT&T Bell Laboratories, Murray Hill, NJ 07974.
T. P. Armstrong and H. T. Choo, Department of Physics, University of Kansas, Lawrence, KS 66045.
R. E. Gold, S. M. Krimigis, E. C. Roelof, The Johns Hopkins University/Applied Physics Laboratory, Laurel, MD 20723.
K. A. Anderson and R. P. Lin, Space Sciences Laboratory, University of California, Berkeley, CA 94720.
M. Pick, Observatoire de Paris, 92195 Meudon Cedex, France.
E. T. Sarris, University of Thrace, Xanthi 67100, Greece.
G. M. Simnett and S. J. Tappin, Department of Space Research, University of Birmingham, Birmingham B15 2TT, United Kingdom.

*To whom correspondence should be addressed.

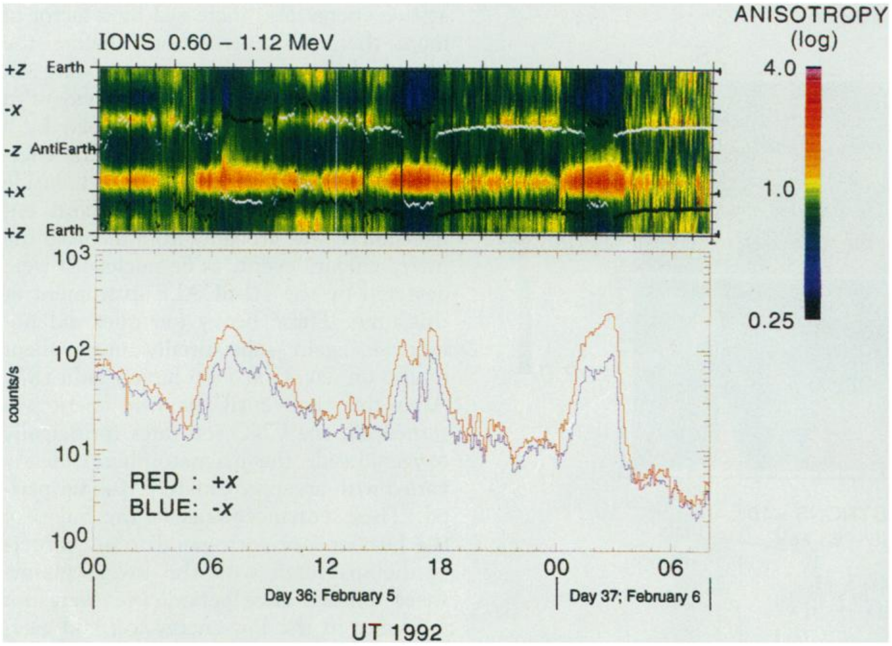

Fig. 2. Details of ion observations in the day-side magnetosphere. (**Upper panel**) Color-coded ion anisotropies (scale on the right) as measured in the spacecraft *x-z* plane, which lies approximately parallel to the equatorial plane of the planet. The black and white lines indicate the components of the magnetic field in the *x-z* plane: field-aligned particles are aligned with the white lines, whereas those particles aligned with the black lines flow opposite the field direction. (**Lower panel**) Counting rates for ions detected in the +*x* sector (red trace) of one of the instrument sensors, a sector that measures particles traveling in the −*x* direction, the direction of the planetary corotation. The blue trace corresponds to particles traveling opposite the corotation direction.

The upper panel of Fig. 2 shows the anisotropy (over 360°) of the ions (0.6 to 1.12 MeV) in the *x-z* plane as a function of time. The information for this plot is derived from four similar detector telescopes that for this presentation are normalized in energy with respect to each other. For each detector, the spin sectors nearest the *x-z* plane are used to derive flux values in eight directions (azimuths) in the *x-z* plane at a specific time. Each of these fluxes is divided by the average (omnidirectional) flux at this time. Linear interpolation is done between these eight anisotropy values, and the resulting anisotropy is color coded and plotted as a strip at the appropriate time. The directions given on the left-hand axis (Fig. 2) are those of the look directions of the sectors. Particles, to be detected, must be moving in the direction opposite the direction in which the detector is looking.

Superimposed on the anisotropies of Fig. 2 are black and white lines that correspond to components of the magnetic field directions in the *x-z* plane as a function of time [magnetic field data are from the Ulysses magnetometer experiment (9)]. The white lines align with particles flowing in the general direction of the magnetic field (field-aligned), whereas the black lines correspond to particles flowing opposite the magnetic field direction. At the approximate center of each of the three enhancements in the particle count rates shown in the figure, the magnetic field direction reverses, indicating a crossing of the Jovian plasma sheet. On average, the particle flow is directed in the −*x* direction (particles detected in the +*x* sector). The anisotropies are larger in the plasma sheet than when the spacecraft is above the sheet where the fluxes are smaller (Fig. 2, lower panel). At times, when the spacecraft is quite far from the plasma sheet, the anisotropies become small and sometimes are even aligned with the magnetic field; these instances are related to plasma flows on the edges of the plasma sheet (6).

Shown in the lower panels of Fig. 3 are ion and electron count rates as a function of time for 3 days of the Ulysses outbound pass at increasing Jovian latitudes on the dusk-

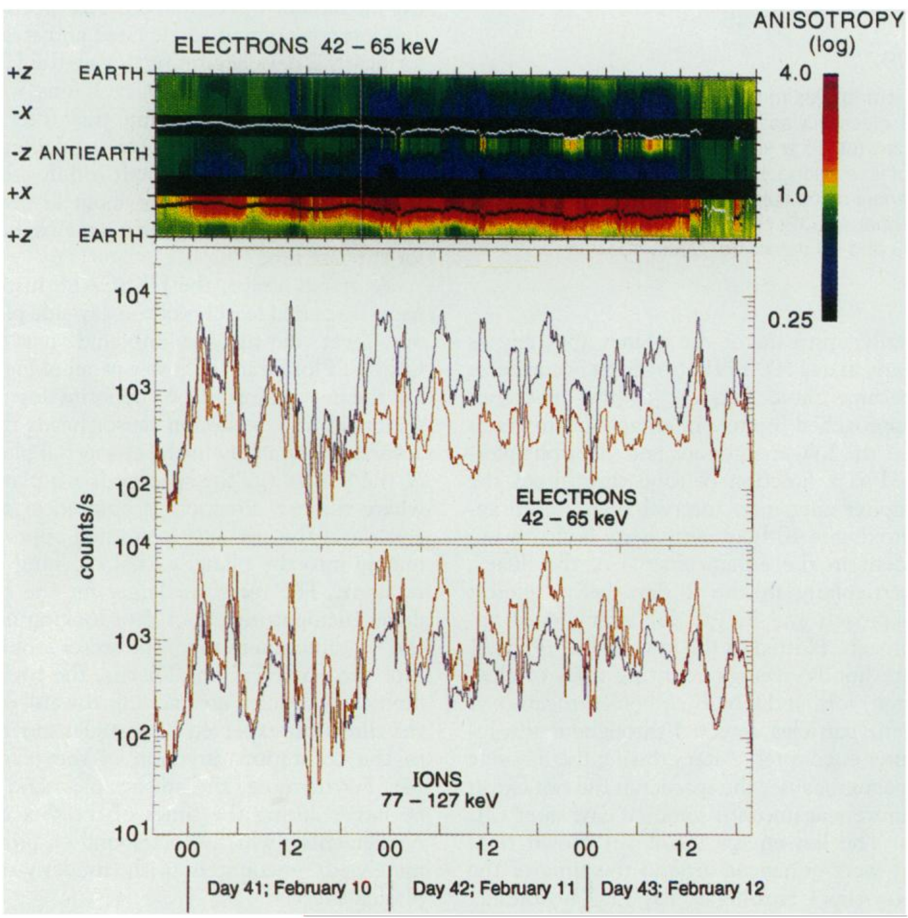

Fig. 3. Details of electron and ion anisotropies during much of the high-latitude outbound pass of Ulysses. (**Upper panel**) A color-coded representation of the electron anisotropies (anisotropy scale to the right) in the *x-z* plane throughout the interval (Fig. 2). The two black swaths correspond to directions in this plane where electron measurements were not made. (**Lower panels**) Electron and ion counting rates throughout the interval in opposite sectors. Hours are indicated at the bottom (UT).

side of the magnetosphere. The two traces shown in each case are the fluxes in opposite sectors measured by the particular detector system at the specific time. In general throughout this entire interval, the anisotropies were quite large and much larger than seen on the day side. During most of the time, all of the sectors for a given detector, with the exception of one or two with the highest counting rates, had rates comparable to that of the lowest rates shown (Fig. 3). That is, the particle fluxes were highly directional and superimposed on an isotropic hot plasma background. Another interesting feature of the count rates is the irregularity in the intensities as a function of time. The irregularities in the magnitudes of the electron and the ion rates tend to track one another. The electron anisotropies remain large for the entire interval, whereas the ion anisotropies most often decrease substantially at the times when the count rates change.

The electron anisotropies shown in the

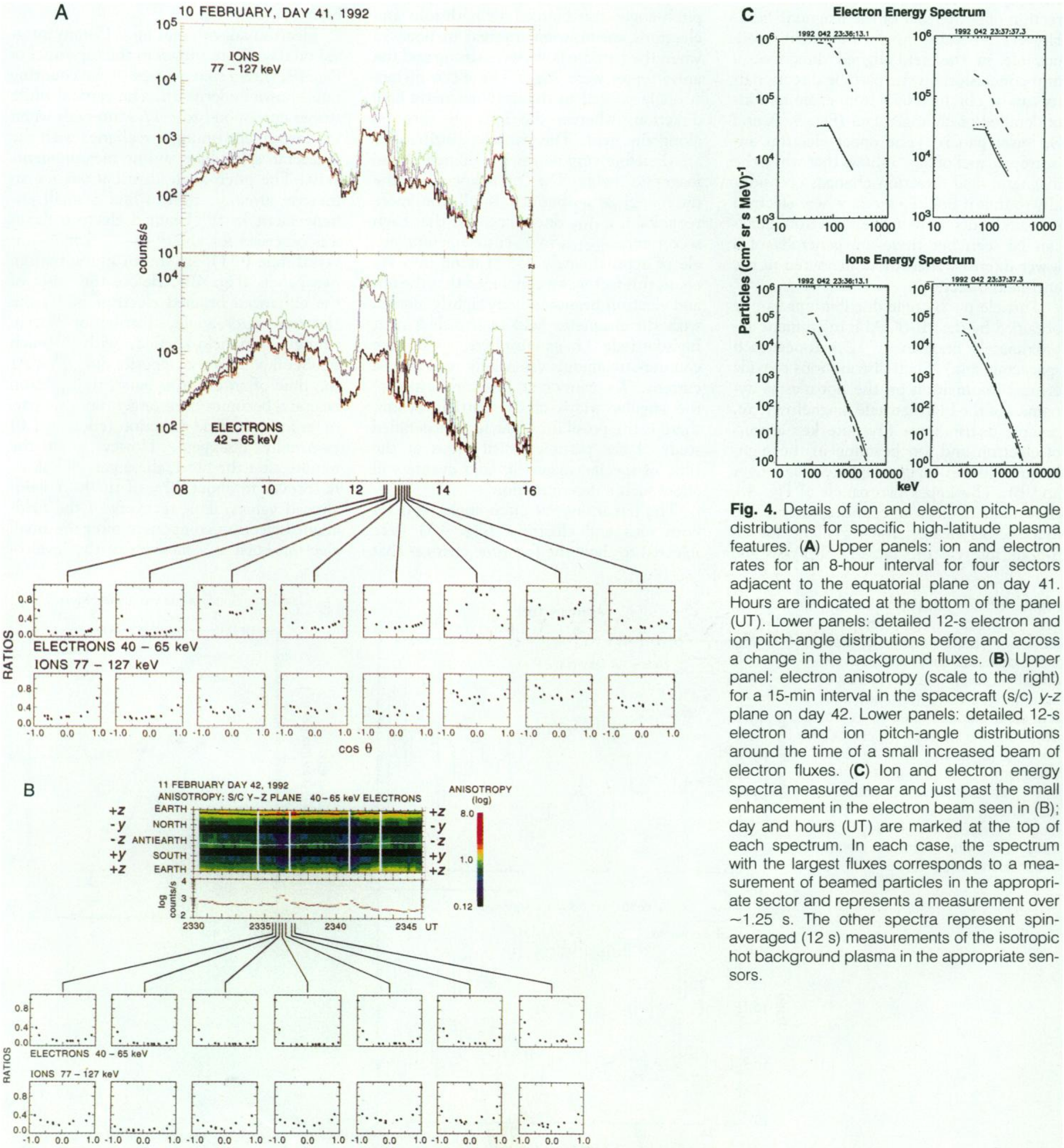

Fig. 4. Details of ion and electron pitch-angle distributions for specific high-latitude plasma features. (**A**) Upper panels: ion and electron rates for an 8-hour interval for four sectors adjacent to the equatorial plane on day 41. Hours are indicated at the bottom of the panel (UT). Lower panels: detailed 12-s electron and ion pitch-angle distributions before and across a change in the background fluxes. (**B**) Upper panel: electron anisotropy (scale to the right) for a 15-min interval in the spacecraft (s/c) *y-z* plane on day 42. Lower panels: detailed 12-s electron and ion pitch-angle distributions around the time of a small increased beam of electron fluxes. (**C**) Ion and electron energy spectra measured near and just past the small enhancement in the electron beam seen in (B); day and hours (UT) are marked at the top of each spectrum. In each case, the spectrum with the largest fluxes corresponds to a measurement of beamed particles in the appropriate sector and represents a measurement over ~1.25 s. The other spectra represent spin-averaged (12 s) measurements of the isotropic hot background plasma in the appropriate sensors.

upper panel of Fig. 3 are in the same format as the ion anisotropies of Fig. 2. The two completely black swaths correspond to directions where no measurements are possible at these energies in this plane. Throughout this entire outbound interval, the magnetic field direction remains relatively unchanged in direction. The anisotropy plot shows that the electron flows are strongly magnetic field–aligned in the direction opposite that of the magnetic field. However, because no measurements were possible in the field-aligned direction, a firm conclusion on the particle directionality can be obtained only from examinations of detailed pitch-angle data (Fig. 4, A and B, lower panels). The upper electron anisotropy panel of Fig. 3 shows that when the magnetic field direction changes occasionally so that it lies in a sector where electron measurements were made, electron fluxes can be seen but these are generally of a lower intensity than those measured in the anti-field direction.

Particle pitch-angle distributions can be obtained by the HI-SCALE instrument approximately once every 12 s (once each spacecraft spin). Such distributions provide critical information on the hot plasma dynamics of the high-latitude magnetosphere. Sample distributions illustrate key aspects of electron and ion beaming in the high-latitude Jovian magnetosphere (Fig. 4, A and B). The upper two panels of Fig. 4A show ion and electron counting rates in the four sectors nearest the x-z plane for an 8-hour interval on day 41. Whereas the fluxes in the two lowest rate sectors track each other very well throughout the interval plotted, those in the two high rate sectors vary in intensity relative to each other. Plotted beneath the counting rate panels (Fig. 4A) are pitch-angle distributions keyed to the time intervals shown in hours 12 and 13 (each distribution is normalized to the maximum flux in the 12-s interval of the distribution). The first two pitch-angle distributions for both ions and electrons are from an interval in hour 12 when the particle flows were strong and the anisotropies were large. The electrons are strongly peaked in the anti–magnetic field direction, whereas the ions are directed along the field. The particle distributions are therefore very narrowly confined by the magnetic field. The narrowness of the pitch-angle distributions is all the more remarkable when one recognizes that each sector corresponds to a sensor opening angle of approximately 45°. Taking into account this factor, we concluded that the ion and electron beams are very tightly aligned with the magnetic field in the dusk-side, high-latitude magnetosphere and are counter-streaming, essentially carrying a current. We cannot at this time estimate the angular width of the particle beams; there is the possibility that further detailed study of the particle distributions at the time of specific magnetic field events will allow such a determination.

The remaining six pitch-angle plots for both ions and electrons (Fig. 4A) were selected to show the fast-time changes that can occur in the distributions as the particle intensities change abruptly. The electron pitch-angle distributions change within minutes from anti–field-aligned to bi-directional to trapped to bi-directional and back to anti–field-aligned. During this time, the ion distributions become more bi-directional. The ions and electrons again become counter-streaming in the interval of large anisotropies during the middle portion of hour 13.

Electron anisotropies for a 15-min interval on day 42 are shown in the top panel of Fig. 4B, with a spin average of the counting rates shown underneath. The vertical white stripes correspond to ~12-s intervals when the instrument timing is realigned with the spacecraft spin phase and no measurements exist. The pitch-angle distributions for an interval around a time when a small enhancement in the beamed electron fluxes was observed for about 45 s [~23:36 universal time (UT)] are shown in the bottom two panels (Fig. 4B). Before the onset of the enhanced beamed electron burst, the electron pitch-angle distributions were strongly anti–field-aligned, with a much smaller flux from the opposite direction. At the time of an electron burst, the electron beaming becomes even larger, and the particles from the field direction ($\cos\theta = 1.0$) essentially disappear. However, in the minute after the burst, these particles slowly recover to about 30% of the anti–field-aligned values. This recovery of the field-aligned electron component after the small electron burst is a measure of the level of

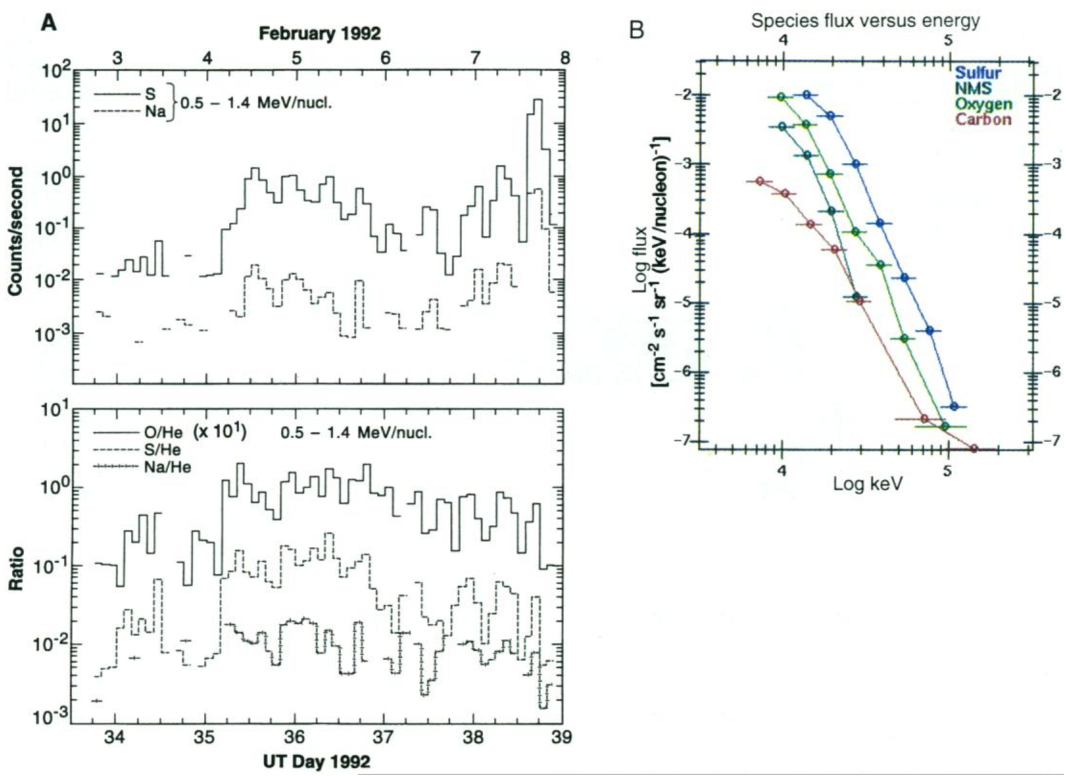

Fig. 5. Ion composition in the Jovian day-side magnetosphere. (**A**) Upper panel: counting rates of the detected sulfur and sodium nuclei. Lower panel: relative abundances of oxygen, sodium, and sulfur nuclei to helium in the day-side magnetosphere. Nucl., nucleon. (**B**) Energy spectra [particles cm^{-2} s^{-1} sr^{-1} (keV/nucleon)$^{-1}$] as a function of particle total energy for four nuclear species measured in the day-side magnetosphere. NMS, neon, magnesium, silicon.

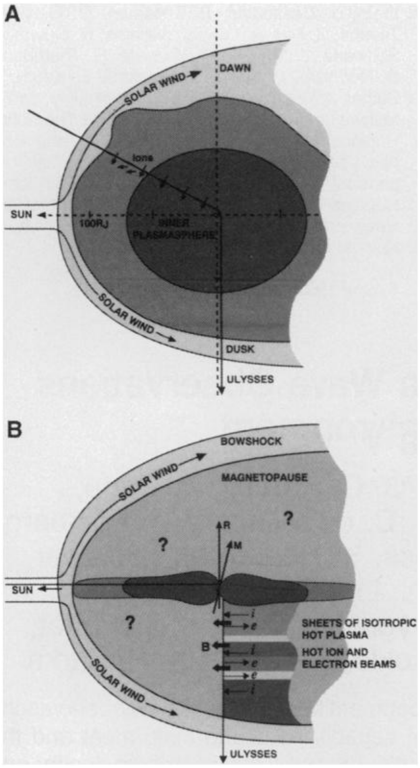

Fig. 6. Plasma model of the Jovian magnetosphere, adapted and changed from the Voyager results (*12*) and incorporating discoveries by the HI-SCALE instrument in the high-latitude, dusk-side magnetosphere. (**A**) The equatorial plane. (**B**) The meridional plane. The model emphasizes the hot plasma regions. Question marks indicate areas of continuing uncertainty; *i*, ions; *e*, electrons; B, planetary magnetic field direction; R, planetary rotation axis; M, planetary dipole magnetic axis.

pitch-angle scattering in the high-latitude magnetosphere or a measure of the distance the electrons travel to a mirror point in the magnetotail, or both. Throughout the interval shown in Fig. 4B, the ion anisotropies remain approximately field-aligned, with an anisotropy at these energies of about 40 to 50% and larger at times. Hence, the electrons and ions are counter-streaming, with small changes occurring occasionally in the anisotropies and in the particle intensities.

Two electron and two ion energy spectra taken at times near the peak and just past the peak of the electron burst at ~23:36 UT on day 42 are shown in Fig. 4C. The spectrum with the highest rates in each panel is from the sector that looks approximately in the direction of the beams at the appropriate times in the spacecraft spin period. The accumulation times for the sector counts are ~1.25 s. The other spectra shown are spin-averaged (~12 s) spectra from detectors that measure the isotropic hot background plasma. It is clear that in the case of the electrons, the beaming particles cover the entire energy range measured. In the case of the ions, the beamed particles cover the range from the lowest energies measured to nearly 1 MeV.

Our detection of the possible presence of anti–field-aligned ions (presumably resulting from reflections or the mirroring of the field-aligned beam closer to Jupiter) is limited by the incomplete angular coverage of the low-energy ion measurements. Often, a very tightly confined beam could have escaped measurement. However, at higher energies, where angular coverage is always complete, there is no evidence of substantial reflected ions, although electron contamination limits the sensitivity of this determination to some extent. In summary, a high-energy reflected ion beam of perhaps 20 to 30% of the field-aligned beam cannot be excluded as a possibility. More detailed analysis will allow this measurement to be further refined.

An estimate has been made of the current density that is carried by the ions and electrons (~50 to 300 keV) in the high-latitude dusk-side magnetosphere from just outside the plasma sheet to the magnetopause. We find a typical current density throughout this region of $\sim 1.6 \times 10^{-4}$ $\mu A/m^2$ or $\sim 8 \times 10^5$ A/R_J^2. The relationships between these current densities and the measured magnetic fields on Ulysses require detailed study.

The composition of the ion population with energies greater than about 0.5 MeV per nucleon was measured throughout the Jovian magnetosphere (Fig. 1). Presented in the top panel of Fig. 5A are the sulfur and sodium (*10*) counting rates as a function of time during the inbound portion of the Ulysses pass, when measurements were made closest to the plasma sheet. The ~10-hour periodicity of the nuclei counting rates is evident, particularly in the sulfur rates. The rates drop during day 37 and then increase substantially as the spacecraft climbs to higher Jovian latitudes before closest approach. In particular, during the last 10-hour plasma increase on day 38, before the instrument was turned off, HI-SCALE measured the largest abundances of both species.

After the sharp increase on day 35 in the abundances of oxygen, sulfur, and sodium ions relative to helium (same energy/nucleon particles) during the inbound trajectory (Fig. 5A) (*10*), the relative abundances remained rather constant for about 2 days. Then these relative abundances dropped for all species, beginning at about 50 R_J. This decrease in the abundances of sulfur and oxygen relative to helium in the inner regions of the magnetosphere is opposite that reported from Voyager measurements of approximately the same energy particles (*11*); it may be related to differences in the latitude dependence of the primarily Io-derived sulfur and oxygen species compared to the latitude dependence of the helium species.

The energy spectra for four of the nuclear species measured in Jupiter's magnetosphere (Fig. 5B) (*10*) are derived from the measurements made in the day-side magnetosphere from 08:00 UT day 35 until the instrument was turned off on day 38.

The HI-SCALE measurements provide unique perspectives on the Jovian magnetosphere, showing definitively that the high-latitude region traversed by Ulysses is dominated by regions of isotropic hot plasma upon which are superimposed essentially continuously flowing beams of counter-streaming hot electrons and ions. The counter-streaming particles essentially fill the entire high-latitude magnetosphere from the edge of the plasma sheet to the dusk-side magnetopause (Fig. 6). This plasma model of the magnetosphere is adapted from that of Krimigis *et al.* (*12*) after their synthesis of data from the two Voyager encounters with the Jovian magnetosphere. Here, we have added the Ulysses trajectory, extending the magnetopause boundary to ~105 R_J and the inner plasmasphere to ~80 R_J, in correspondence with the Ulysses observations and in contrast to the Voyager LECP-determined day-side boundaries at ~75 R_J and ~50 R_J for the magnetopause and the inner boundary, respectively. Consistent with the Voyager results, we find the hot plasma in the day-side magnetosphere to be moving in the corotational direction, with the largest anisotropies occurring near the center portions of the plasma sheet. Although the Ulysses hot ion measurements were not made at as low an energy as the Voyager measurements, we find the hot ion energy densities in the plasma sheet to be approximately sufficient to balance the magnetic energy densities.

On the dusk side at high latitudes (Fig. 6), the hot plasma particles are counter-streaming and carry a current density of ~8 $\times 10^5$ A/R_J^2. The strong and persistent field-aligned currents are superimposed on an isotropic hot background plasma that is variable in time; at the boundaries between the plasma regimes, the particle distributions can be quite mixed for time intervals of a few tens of seconds to minutes. The field-aligned particle beams are tightly confined to magnetic field lines that appear to be swept strongly tailward. The high-latitude magnetosphere thus appears to be dominated by solar wind interaction with the planet's magnetic field.

The HI-SCALE particle pitch-angle distributions were examined in some detail in intervals of several hours before and after instrument turn-off around closest approach. Using these distributions and a model of the Jupiter ionosphere, we can conservatively conclude that the energy input into the Jovian aurora (*13*) by the measured electrons in the loss cone at a latitude (λ) of $\sim 20°$ is ~ 1.0 erg cm^{-2} s^{-1} and the ion input is about a factor of 10 less (*14*). Furthermore, the discovery of the ion and electron particle beams throughout the high-latitude magnetosphere suggests that at least a portion of these particles (whose loss cones at the locations where they are measured are only a small fraction of a degree) can also be lost into the ionosphere and produce polar cap auroras on the planet. That some loss must occur is evident from the pitch-angle distributions, whereas the particle beams are strongly unidirectional, with only a small component seen in the backscattered direction for both ions and electrons.

REFERENCES AND NOTES

1. L. J. Lanzerotti *et al.*, *Astron. Astrophys. Suppl. Ser.* **92**, 349 (1992).
2. Extensive summaries of the studies of the Jovian magnetosphere made by the Pioneer and Voyager spacecraft are included in special issues of the *Journal of Geophysical Research* [**79** (1 September 1974); **86** (30 September 1981)] and in *Physics of the Jovian Magnetosphere*, A. J. Dessler, Ed. (Cambridge Univ. Press, Cambridge, 1983).
3. The HI-SCALE instrument consists of five separate detector apertures in two separate telescope assemblies that are mounted by means of individual stub arms on a box containing the electronics. The instrument is mounted on one corner of the Ulysses spacecraft in order to provide unimpeded fields-of-view to the telescopes. Four of the detector apertures consist of back-to-back magnetic and foil spectrometers to separate electrons and ions. The composition aperture (CA) telescope provides a multiparameter separation of individual nuclear species. The energy passbands and orientations of the magnetic-foil spectrometers are such that a nearly complete 4π coverage of the solid angle is possible over a wide range of electron and ion energies. Unfortunately, some design compromises in the early stages of the instrument development, mandated during project definition, prevented some regions of angle–energy phase space from being covered.
4. S. M. Krimigis *et al.*, *J. Geophys. Res.* **86**, 8227 (1981).
5. R. D. Zwickl *et al.*, *ibid.*, p. 8125.
6. L. J. Lanzerotti *et al.*, in preparation.
7. The spacecraft locations during the Jupiter encounter are presented in an overview in this issue [E. J. Smith, K.-P. Wenzel, D. E. Page, *Science* **257**, 1503 (1992)].
8. L. J. Lanzerotti *et al.*, data not shown.
9. A. Balogh *et al.*, *Astron. Astrophys. Suppl. Ser.* **92**, 221 (1992).
10. The counting rates for the nuclei denoted as sodium or neon, magnesium, silicon (NMS) or both herein can include counts from other nuclei such as silicon and magnesium as well. However, because the abundances of these species in the Jovian magnetosphere are expected to be very low, we believe that essentially all of the rates we denote here as sodium are indeed sodium.
11. D. C. Hamilton *et al.*, *J. Geophys. Res.* **86**, 8301 (1981).
12. S. M. Krimigis *et al.*, *Science* **206**, 977 (1979).
13. A. L. Broadfoot *et al.*, *J. Geophys. Res.* **86**, 8259 (1981).
14. After the Pioneer and Voyager measurements of near-equatorial particles in the inner Jovian magnetosphere, there were extensive theoretical discussions of particle loss processes into the planet's atmosphere. See R. M. Thorne, in *Physics of the Jovian Magnetosphere*, A. J. Dessler, Ed. (Cambridge Univ. Press, Cambridge, 1983), pp. 454–488.

15. We express great thanks to our colleagues A. Balogh, Principal Investigator and R. Forsyth, Co-Investigator on the magnetometer team for sharing their data with us. We thank many people at our home institutions for their design, engineering, and software support over many years on behalf of this investigation, including R. Weitzmann, R. Campbell, R. Williams, D. Curtis, W. Frain, J. Dassoulas, B. Tossman, S. Gary, C. Tielens, D. Fort, A. Lew, S. Williams, D. Guynn, P. Schwartz, J. Mueller, C. Wingate, R. Thompson, B. Northrup, L. Staub, E. Hawkins, E. Keath, L. Suther, J. Townsend, K. Parker, G. Shelley, and L. Manweiler. The work on HI-SCALE at The Johns Hopkins University/Applied Physics Laboratory has been supported by NASA under Task I of contract N00039-89-C-0001 between The Johns Hopkins University and the Department of the Navy and by subcontract at the University of Kansas and the University of California.

1 June 1992; accepted 7 August 1992

Ulysses Radio and Plasma Wave Observations in the Jupiter Environment

R. G. Stone, B. M. Pedersen, C. C. Harvey, P. Canu, N. Cornilleau-Wehrlin, M. D. Desch, C. de Villedary, J. Fainberg, W. M. Farrell, K. Goetz, R. A. Hess, S. Hoang, M. L. Kaiser, P. J. Kellogg, A. Lecacheux, N. Lin, R. J. MacDowall, R. Manning, C. A. Meetre, N. Meyer-Vernet, M. Moncuquet, V. Osherovich, M. J. Reiner, A. Tekle, J. Thiessen, P. Zarka

The Unified Radio and Plasma Wave (URAP) experiment has produced new observations of the Jupiter environment, owing to the unique capabilities of the instrument and the traversal of high Jovian latitudes. Broad-band continuum radio emission from Jupiter and in situ plasma waves have proved valuable in delineating the magnetospheric boundaries. Simultaneous measurements of electric and magnetic wave fields have yielded new evidence of whistler-mode radiation within the magnetosphere. Observations of auroral-like hiss provided evidence of a Jovian cusp. The source direction and polarization capabilities of URAP have demonstrated that the outer region of the Io plasma torus supported at least five separate radio sources that reoccurred during successive rotations with a measurable corotation lag. Thermal noise measurements of the Io torus densities yielded values in the densest portion that are similar to models suggested on the basis of Voyager observations of 13 years ago. The URAP measurements also suggest complex beaming and polarization characteristics of Jovian radio components. In addition, a new class of kilometer-wavelength striated Jovian bursts has been observed.

The unique configuration, wide frequency range, and high sensitivity of the URAP instrument (*1*) have allowed many new observations to be made of both in situ and remote phenomena during the Ulysses-Jupiter encounter in early February 1992. The spacecraft's trajectory through high-latitude regions provided access to magnetospheric regions and radio source viewing geometries not available on previous missions (*2*). In addition, because of the retrograde nature of the trajectory, a large range of Jovian longitudes was surveyed during closest approach (CA), and the outbound trajectory was toward the Jovian dusk terminator.

The URAP sensors consist of a spin plane electric field dipole antenna (E_x), a spin axis electric field monopole antenna (E_z), and two magnetic search coils (B_y and B_z). The electric field measurements covered the frequency range from dc to 940 kHz, and the magnetic field measurements covered the frequency range from 0.08 to 448 Hz. The combination of magnetic and electric sensors made possible the first investigation of the electromagnetic nature of Jovian low-frequency emissions. The Ulysses radio astronomy receivers were specifically designed to measure simultaneously both the direction and the complete polarization state of a remote radio source. An active sounder provided additional in situ plasma measurements during the crossing of the Io torus.

R. G. Stone, M. D. Desch, J. Fainberg, W. M. Farrell, M. L. Kaiser, R. J. MacDowall, National Aeronautics and Space Administration Goddard Space Flight Center, Greenbelt, MD 20771.
B. M. Pederson, C. C. Harvey, S. Hoang, A. Lecacheux, R. Manning, N. Meyer-Vernet, M. Moncuquet, P. Zarka, Observatoire de Paris-Meudon, 92195 Meudon Principal Cedex, France.
P. Canu, N. Cornilleau-Wehrlin, C. de Villedary, Centre de Recherches en Physique de l'Environnement Terrestre et Planetaire (CRPE) CRPE/CNET/CNRS, 92131 Issy-les Moulineaux, France.
K. Goetz, P J. Kellogg, N. Lin, J. Thiessen, School of Physics and Astronomy, University of Minnesota, Minneapolis, MN 55455.
R. A. Hess, C. A. Meetre, V. Osherovich, M. J. Reiner, A. Tekle, Hughes STX, Lanham, MD 20706.